

Observation of Devil's Staircase in the Novel Spin Valve System $\text{SrCo}_6\text{O}_{11}$

T. Matsuda,¹ S. Partzsch,² T. Tsuyama,^{1,3} E. Schierle,⁴ E. Weschke,⁴
J. Geck,² T. Saito,⁵ S. Ishiwata,¹ Y. Tokura,^{1,6} and H. Wadati^{1,3,*}

¹*Department of Applied Physics and Quantum-Phase Electronics Center (QPEC),
University of Tokyo, Hongo, Tokyo 113-8656, Japan*

²*Leibniz Institute for Solid State and Materials Research IFW Dresden, Helmholtzstrasse 20, 01069 Dresden, Germany*

³*Institute for Solid State Physics, University of Tokyo, Kashiwanoha 5-1-5, Chiba 277-8581, Japan*

⁴*Helmholtz-Zentrum Berlin für Materialien und Energie, Albert-Einstein-Str.15, 12489 Berlin, Germany*

⁵*Institute for Chemical Research, Kyoto University, Uji, Kyoto 611-0011, Japan*

⁶*RIKEN Center for Emergent Matter Science (CEMS), Wako, Saitama 351-0198, Japan*

(Dated: December 30, 2014)

Using resonant soft x-ray scattering as a function of both temperature and magnetic field, we reveal a large number of almost degenerate magnetic orders in $\text{SrCo}_6\text{O}_{11}$. The Ising-like spins in this frustrated material in fact exhibit a so-called magnetic devil's staircase. It is demonstrated how a magnetic field induces transitions between different microscopic spin configurations, which is responsible for the magnetoresistance of $\text{SrCo}_6\text{O}_{11}$. This material therefore constitutes a unique combination of a magnetic devil's staircase and spin valve effects, yielding a novel type of magnetoresistance system.

PACS numbers: 71.30.+h, 71.28.+d, 79.60.Dp, 73.61.-r

Combining different materials in artificial nanostructures is a most important approach to create improved or even completely new electronic functionalities for technological applications. A very prominent example for this is the giant magnetoresistance (GMR), which was first realized by multilayers of alternating nonmagnetic and ferromagnetic metals [1, 2] and which now is an indispensable part of today's information technology. In these GMR systems the electrical resistance is high for an antiparallel alignment of the magnetization in the neighboring magnetic layers, while it is low for a parallel alignment of those magnetizations. For this reason such systems are also referred to as spin valves.

Large or even colossal magnetoresistance can also occur as an intrinsic effect in bulk materials, due to the interplay of mobile charge carriers and localized spins. Here the doped manganites provide the probably most famous examples [3–7]. A particularly interesting material with intrinsic magnetoresistance is the recently discovered Co oxide $\text{SrCo}_6\text{O}_{11}$, the lattice structure of which is believed to realize a GMR multilayer system at the atomic scale [8]. Figure 1 (a) shows the normalized out-of-plane resistivity $\rho_c(H)/\rho_c(0)$ of $\text{SrCo}_6\text{O}_{11}$ ($H//c$), which is a clear manifestation of magnetoresistance in this material [9]. As shown in Fig. 1 (b), $\text{SrCo}_6\text{O}_{11}$ exhibits a layered crystal structure consisting of three parts: (i) metallic Kagome-layers formed by the edge-sharing octahedra, (ii) dimerized octahedra and (iii) trigonal bipyramids. In the following the Co-sites of the Kagome-layers, the dimerized octahedra and trigonal bipyramids are referred to as Co(1), Co(2) and

Co(3), respectively (cf. Fig. 1 (b)). It was shown earlier that the magnetism of $\text{SrCo}_6\text{O}_{11}$ is due to localized Ising-like spins of the Co(3)-sites, whereas the charge transport happens in the subsystems containing Co(1) and Co(2) [9]. The metallic Kagome-layers are hence linked by magnetic layers containing Co(3) and therefore realize a GMR-multilayer structure at the atomic level. The observed strong Ising type anisotropy along the c axis can be explained by a non-vanishing orbital moment and the resulting spin-orbit coupling of Co(3), as discussed earlier for $\text{Ca}_3\text{Co}_2\text{O}_6$, which also contains Co-sites with trigonal local symmetry [10].

One of the most striking magnetic features of $\text{SrCo}_6\text{O}_{11}$ observed so far are plateaus in the magnetization as a function of the applied magnetic field along the c -axis [8] as shown in Fig. 1 (c). These plateaus correspond to $1/3$ and $3/3$ of the saturated moment [8] and were found to reflect different stackings along c , namely an up-up-up structure for the $3/3$ phase and an up-up-down configuration for the $1/3$ phase [11]. As in the case of an artificial GMR-multilayer, the transition between these magnetic phases are thought to cause the giant magnetoresistance of this compound. Specifically, the magnetic up-up-up structure of the $3/3$ phase [9] leads to less spin scattering and therefore a smaller electrical resistivity than in the up-up-down configuration of the $1/3$ phase [9].

In this letter, we present a high-resolution resonant soft x-ray scattering (RSXS) study of $\text{SrCo}_6\text{O}_{11}$ bulk single crystals as a function of temperature (T) and applied magnetic field (H). We discover various metastable magnetic orders in low magnetic fields that escaped detection in earlier experiments. The occurrence of all these metastable phases can be interpreted in terms of strong frustration in a strongly anisotropic magnetic system, which results in a large variety of almost degenerate magnetic structures [12–19]. In fact, our results im-

*Electronic address: wadati@issp.u-tokyo.ac.jp;
URL: <http://www.geocities.jp/qxbqd097/index2.htm>

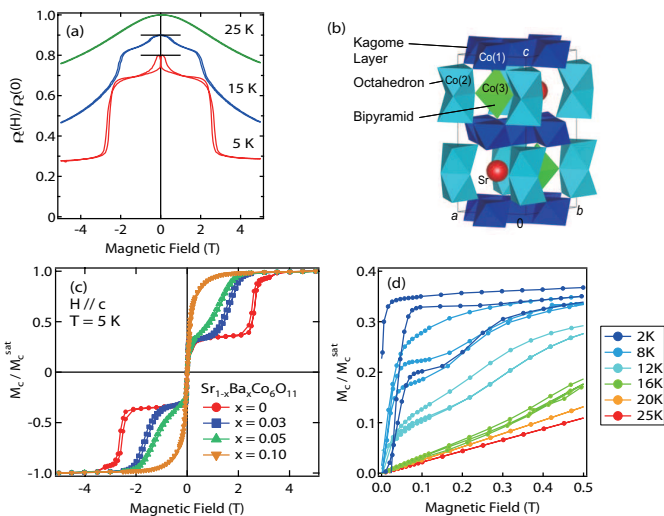


FIG. 1: (Color online) (a) Normalized out-of-plane resistivity $\rho_c(H)/\rho_c(0)$ of $\text{SrCo}_6\text{O}_{11}$ ($H//c$) taken from Ref. [9]. (b) Crystal structure of $\text{SrCo}_6\text{O}_{11}$. (c) Out-of-plane magnetization of $\text{Sr}_{1-x}\text{Ba}_x\text{Co}_6\text{O}_{11}$ as a function of magnetic field ($H//c$) at 5 K. (d) Temperature dependence of out-of-plane magnetization of $\text{SrCo}_6\text{O}_{11}$ in low magnetic field region ($H//c$).

ply that $\text{SrCo}_6\text{O}_{11}$ is the first realization of a magnetic devil's staircase in a $3d$ -electron system. Our central result therefore is that magnetic frustration is a fundamental ingredient for the functionality of $\text{SrCo}_6\text{O}_{11}$ which realizes a novel and sensitive GMR-system at the atomic level in a single phase material. In addition, the high degree of frustration intrinsically causes a strong sensitivity of the system to external modifications which consequently opens the possibility of tailoring functionality as demonstrated in this study by Ba substitution at the Sr site.

Pure and Ba-substituted $\text{SrCo}_6\text{O}_{11}$ bulk single crystals were synthesized by the high-pressure technique [8]. The typical sample size was $\simeq 0.20 \times 0.20 \times 0.05 \text{ mm}^3$. The out-of-plane magnetization of pure and Ba-substituted $\text{SrCo}_6\text{O}_{11}$ are shown in Figs. 1 (c) and (d). RSXS is a powerful tool to reveal ordered structures in solids such as magnetic, charge and orbital ordering [20–25]. Here we employed the strongly enhanced magnetic sensitivity of RSXS at the Co $2p_{3/2}$ edge (780 eV) in order to investigate the subtle magnetic phase transitions in our small-volume samples depending on temperature and external magnetic fields. The present study is one of the very first RSXS experiments performed under magnetic fields of several Tesla. The experiments were carried out at the High-field Diffractometer operated at the UE46-PGM1 beamline of BESSY-II, Germany. Figure 2 (a) shows the scattering geometry used for the present experiments. Temperatures down to 4 K could be reached using a continuous helium-flow cryostat. X-ray polarization was linear (σ and π). Applied magnetic field was up

to 4 T.

Figure 2 (b) shows the diffraction peaks of $\text{SrCo}_6\text{O}_{11}$ at zero field for various temperatures. Quite surprisingly and very uncommon for RSXS experiments, a large number of superlattice reflections at $L = 2/3, 5/6, 1, 7/6, 4/3$ and $3/2$ is observed. The small and temperature independent peak at $L = 1.37$ is assigned to some impurity in the sample because it does not show temperature dependence. $L = 1$ commensurate (CM) peak and two incommensurate (ICM) peaks around $L = 0.8, 1.2$ appear at 20 K (T_{c1}). These ICM peaks move to $L = 5/6$ and $7/6$, respectively, as the temperature is decreased, and finally are locked at these values at 12 K (T_{c2}), respectively. At T_{c2} , there appear $L = 5/6$ and $8/7$ shoulders of the $L = 7/6$, and simultaneously $L = 2/3, 4/3$ and $3/2$ peaks.

Intensities of all the magnetic peaks were independent of the polarizations σ and π , as shown in Fig. 2 (d) for the case of $L = 6/5$. For a trigonal local symmetry and spins along the c direction, the magnetic scattering factor can be expressed as

$$f_{mag} = \frac{\sigma'}{\pi'} \begin{pmatrix} \sigma & \pi \\ 0 & m_c \sin \theta \\ m_c \sin \theta & 0 \end{pmatrix}$$

where m_c is the components of the spins along the c -axis and θ is the scattering angle [26, 27]. In this case, pure $\sigma - \pi'$ and $\pi - \sigma'$ channels have the same intensity, which agrees very well with our experimental results and verifies the interpretation in terms of magnetic scattering.

The emergence of the magnetic $L = 2/3$ and $4/3$ peaks agrees well with the powder neutron diffraction measurement at 2 T. In order to assign the shoulder peaks around $L = 7/6$, the data were fitted by three components of $L = 7/6, 8/7$ and $6/5$ as shown in Fig. 2 (c). These results therefore directly reveal that a large number of magnetic phases coexist in zero magnetic field and, in particular that the $\uparrow\uparrow\downarrow$ configuration is realized even at zero magnetic field. We observed the magnetic peaks of $L = n/6$ with $n = 4, 5, 6, 7, 8$, and 9. However, the temperature dependence varies for different n and the peaks with $n = 5$ and 7 show the shift from ICM to CM peak position and the others do not. This indicates that all the different peaks cannot be due to one magnetic modulation with $L = 1/6$ but belong to different magnetic stacking sequences. This is also reflected in the observed field dependent behaviour.

The geometry of x-ray beam and the superconducting magnet for the field-dependent experiment is shown in Fig. 3 (a). Figure 3 (b) shows the magnetic peaks at 12 K around $L = 4/5$. The denoted values of the magnetic field are the c -axis component because the ab component is irrelevant to the magnetic structures due to the strong Ising-like anisotropy [9, 11]. The $L = 5/6$ peak has strong intensity around $H = 0$ T, while the $4/5$ peak is stabilized around $H = 0.2$ T, indicating that the magnetic peaks with different L behave differently under magnetic fields.

In this way, we have been able to explore the entire H - T diagram of this complex magnetic system as shown

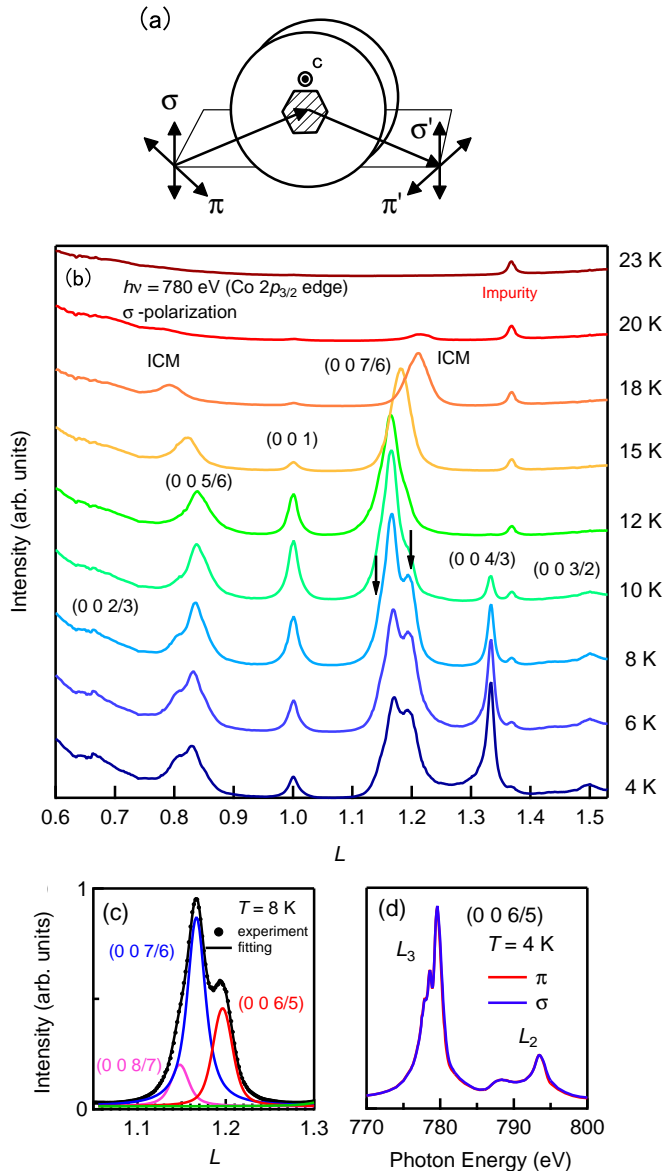


FIG. 2: (Color online) (a) Experimental geometry for RSXS measurements. The arrows indicate the directions of polarizations of x-rays. (b) Magnetic peak profile of $\text{SrCo}_6\text{O}_{11}$ at various temperatures at zero magnetic field. (c) Magnetic peak fitting of $\text{SrCo}_6\text{O}_{11}$ around $L = 7/6$. (d) Photon-energy dependence of intensity of the $L = 6/5$ reflection for σ and π polarizations.

in Fig. 4. The phase boundary between $\uparrow\uparrow\uparrow$ and $\uparrow\uparrow\downarrow$ states was determined by magnetization measurements, and the other boundaries were determined by the present RSXS results. Here, $\langle n \rangle$ represents the magnetic periodicities. Since the $\text{SrCo}_6\text{O}_{11}$ unit cell contains two equivalent Co(3) Bragg planes along c , (002) is the first allowed structural reflections and (001) corresponds to a simple $\uparrow\downarrow\uparrow$ antiferromagnetic order. Therefore $\langle 2 \rangle$ corresponds

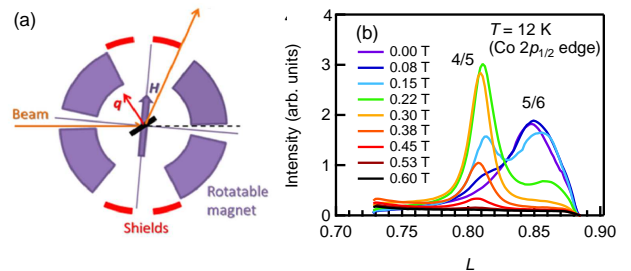


FIG. 3: (Color online) Geometry for RSXS under magnetic field (a), and magnetic peaks observed under various field (b).

to $L = 1, \langle 4 \rangle$ to $L = 3/2, \langle 5 \rangle$ to $L = 4/5$, and $\langle 12 \rangle$ to $L = 5/6$. The phase diagram demonstrates that various magnetic orderings with different periodicities are formed in the low temperature and low field region. Obviously, the energies of these magnetic structures are quite close, and the corresponding energy differences sensitively depend on temperature and magnetic fields. A similar behavior has been observed in CeSb , which also has various magnetic orderings depending on temperature and field [12–14]. This phenomenon is called “the devil’s staircase”, whose mechanism is described by the axial next nearest Ising (ANNNI) model [12–19]. The ANNNI model describes competing interactions between nearest and next-nearest Ising spins, which yields various magnetic orderings with close energies.

In SrCo_6O_6 the situation is very similar in that i) Co(3) has a strong Ising anisotropy and ii) our RSXS results reveal a coexistence of various essentially degenerate magnetic phases. We therefore conclude that the $\text{SrCo}_6\text{O}_{11}$ indeed exhibits a devil’s-staircase scenario, i.e. a coexistence of a large number of magnetic periodicities with almost the same energies. Such coexistence is destroyed by the application of an external magnetic field, selecting only those phases which are energetically favorable now, leading to the magnetization plateaus observed in macroscopic measurements. Therefore, $\text{SrCo}_6\text{O}_{11}$ is considered as the first example of the devil’s staircase which was found in a $3d$ -electron spin system.

However, in order to explain ordered structures with long periodicities, one needs magnetic interactions that go well beyond the nearest neighbors. A plausible explanation can be provided by the Ruderman-Kittel-Kasuya-Yosida (RKKY) interaction via the metallic planes. $\text{SrCo}_6\text{O}_{11}$ has strong coupling between conduction electrons and localized spins, where RKKY interactions play the most important role. Consequently the very complex behaviour of the magnetically highly frustrated $\text{SrCo}_6\text{O}_{11}$ is far beyond the description of the simple ANNNI model. It may be better described by a more complex model with both localized spins and conduction electrons.

Interestingly the observed very complex microscopic

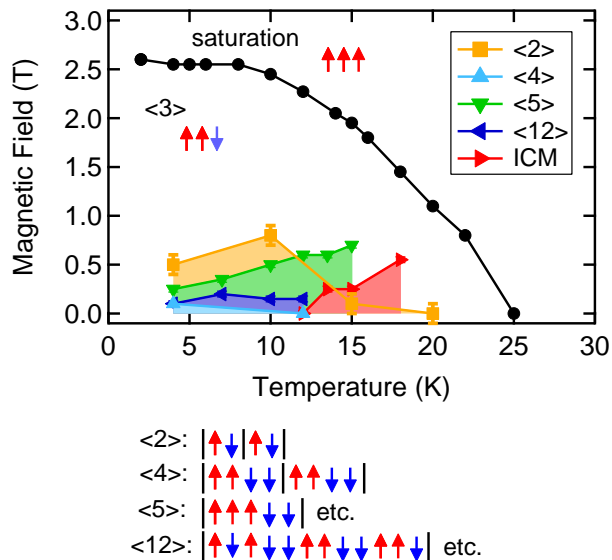


FIG. 4: (Color online) Magnetic phase diagram of $\text{SrCo}_6\text{O}_{11}$ determined by RSXS measurements. The phase boundary between $\uparrow\uparrow\uparrow$ and $\uparrow\uparrow\downarrow$ states was determined by magnetization measurements.

magnetic behavior seems to be also reflected in the macroscopic material properties: The out-of-plane magnetization at low temperatures in low magnetic fields in Fig. 1 (d) show hysteresis and additional plateaus around $1/5$ and $1/6$. These plateaus are caused by the phases of $L = 4/5$ and $5/6$, which have a smaller magnetization than the $1/3$ phase. However, finally, the strongest ferromagnetic phase ($L = 4/3$) is the only remaining phase in higher magnetic fields, which creates the $1/3$ magnetization plateau. This field- and temperature dependent magnetization is closely linked to the measured normalized out-of-plane resistivity $\rho_c(H)/\rho_c(0)$, which is characterized by several plateaus and hysteretic behaviour in the low-field region as shown in Fig. 1 (a). These macroscopic properties can be easily understood on the basis of the observed magnetic phase diagram: The magnetic phases in the low-field region are connected with anomalies in magnetization and resistivity since the magnetic field is able to select and stabilize single phases out of this “nearly degenerate ground state”. Hence, the basic mechanism behind functionality of the novel spin valve system $\text{SrCo}_6\text{O}_{11}$ is a very high degree of magnetic frustration leading to a complex magnetic phase mixture whose delicate balance can be easily modified even by small magnetic fields.

Besides the related magneto-resistive functionality, frustrated magnets are also very sensitive to chemical doping. In contrast to robust systems, which require substantial doping to alter material properties, here a fine tuning of material properties should be possible by very low doping, in this way preventing unwanted side-effects. This is demonstrated in the present study by Ba substi-

tution of Sr of only a few percent as shown in Fig. 5. In $\text{Sr}_{0.97}\text{Ba}_{0.03}\text{Co}_6\text{O}_{11}$ one cannot see any magnetic peaks around $L = 5/6$ or $7/6$, demonstrating that small Ba substitution of only 3% destroys almost the degenerate ground states, and consequently shifts the $1/3 \rightarrow 3/3$ functional step to lower magnetic fields. Stronger substitution of 10% shifts this step to 0 T, i.e. the system has a FM ground state as shown in Fig. 1 (c).

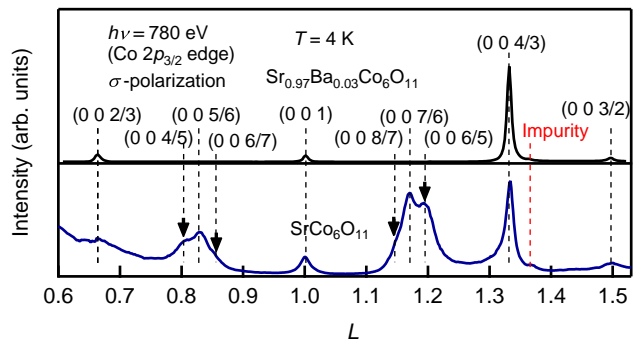


FIG. 5: (Color online) Magnetic peaks at zero field of $\text{SrCo}_6\text{O}_{11}$ and $\text{Sr}_{0.97}\text{Ba}_{0.03}\text{Co}_6\text{O}_{11}$ at 4 K.

In summary, we have investigated the magnetic structures of $\text{SrCo}_6\text{O}_{11}$ bulk single crystals. We observed the first devil’s staircase behavior in a $3d$ system where coupling is mediated by RKKY interaction. This is a consequence of a highly frustrated magnetic systems. The ground state, where there is a coexistence of various magnetic periodicities with almost the same energies, is very susceptible to magnetic fields and finally is the responsible mechanism behind the observed macroscopic functionality. In connection with the layered structure and Ising like anisotropy, this generates a spin valve functionality in a single phase material, which usually requires complex heterostructures. Furthermore, having frustration as the fundamental mechanism, this system can be easily tunable, rising the hope for engineered system properties, which has been demonstrated here by studying the behavior depending on very small amount of Ba doping.

This work was supported by the Japan Society for the Promotion of Science (JSPS) through the “Funding Program for World-Leading Innovative R&D on Science and Technology (FIRST Program)” initiated by the Council for Science and Technology Policy (CSTP) and in part by JSPS Grant-in-Aid for Scientific Research(S) No. 24224009. This work was also partially supported by the Ministry of Education, Culture, Sports, Science and Technology of Japan (X-ray Free Electron Laser Priority Strategy Program) and by a research granted from The Murata Science Foundation. S. P. and J. G. thank the DFG for the support through the Emmy Noether Program (Grant GE 1647/2-1).

-
- [1] M. N. Baibich, J. M. Broto, A. Fert, F. N. Van Dau, F. Petroff, P. Etienne, G. Creuzet, A. Friederich, and J. Chazelas, *Phys. Rev. Lett.* **61**, 2472 (1988).
- [2] G. Binasch, P. Grünberg, F. Saurenbach, and W. Zinn, *Phys. Rev. B* **39**, 4828 (1989).
- [3] A. P. Ramirez, *J. Phys.: Condens. Mat.* **9**, 8171 (1997).
- [4] C. N. R. Rao, A. Arulraj, A. K. Cheetham, and B. Raveau, *J. Phys.: Condens. Mat.* **12**, R83 (2000).
- [5] W. Prellier, P. Lecoeur, and B. Mercey, *J. Phys.: Condens. Mat.* **13**, R915 (2001).
- [6] A. M. Haghiri-Gosnet and J. P. Renard, *J. Phys. D: Appl. Phys.* **36**, R127 (2003).
- [7] Y. Tokura, *Rep. Prog. Phys.* **69**, 797 (2006).
- [8] S. Ishiwata, D. Wang, T. Saito, M. Takano, *Chem. Mater.* **17**, 2789 (2005).
- [9] S. Ishiwata, I. Terasaki, F. Ishii, N. Nagaosa, H. Mukuda, Y. Kitaoka, T. Saito and M. Takano, *Phys. Rev. Lett.* **98**, 217201 (2007).
- [10] H. Wu, M. W. Haverkort, Z. Hu, D. I. Khomskii, and L. H. Tjeng, *Phys. Rev. Lett.* **95**, 186401 (2005).
- [11] T. Saito, A. Williams, J. P. Attfield, T. Wuernisha, T. Kamiyama, S. Ishiwata, Y. Takeda, Y. Shimakawa and M. Takano, *J. Magn. Magn. Mater.* **310**, 1584 (2007).
- [12] P. Bak, *Rep. Prog. Phys.* **45**, 587 (1982).
- [13] J. R.-Mignod, P. Burlet, J. Villain, H. Bartholin, Wang Tcheng-Si, D. Florence and O. Vogt, *Phys. Rev. B* **16**, 440 (1977).
- [14] J. R.-Mignod, J. M. Effantin, P. Burlet, T. Chattopadhyay, L. P. Regnault, H. Bartholin, C. Vettier, O. Vogt, D. Ravot and J. C. Achart, *J. Magn. Magn. Mater.* **52**, 111 (1985).
- [15] K. Ohwada, Y. Fujii, N. Takesue, M. Isobe, Y. Ueda, H. Nakao, Y. Wakabayashi, Y. Murakami, K. Ito, Y. Amemiya, H. Fujihisa, K. Aoki, T. Shobu, Y. Noda, and N. Ikeda, *Phys. Rev. Lett.* **87**, 086402 (2001).
- [16] J. von Boehm and P. Bak, *Phys. Rev. Lett.* **42**, 122 (1979).
- [17] P. Bak and J. von Boehm, *Phys. Rev. B* **21**, 5297 (1980).
- [18] W. Selke and P. M. Duxbury, *Z. Phys. B: Cond. Matt.* **57**, 49 (1984).
- [19] K. Nakanishi, *J. Phys. Soc. Jpn.* **58**, 1296 (1989).
- [20] J. Fink, E. Schierle, E. Weschke and J. Geck, *Rep. Prog. Phys.* **76**, 056502 (2013).
- [21] H. Wadati, J. Okamoto, M. Garganourakis, V. Scagnoli, U. Staub, Y. Yamasaki, H. Nakao, Y. Murakami, M. Mochizuki, M. Nakamura, M. Kawasaki, and Y. Tokura, *Phys. Rev. Lett.* **108**, 047203 (2012).
- [22] S. Partzsch, S. B. Wilkins, J. P. Hill, E. Schierle, E. Weschke, D. Souptel, B. Büchner, and J. Geck, *Phys. Rev. Lett.* **107**, 057201 (2011).
- [23] S. Y. Zhou, Y. Zhu, M. C. Langner, Y.-D. Chuang, P. Yu, W. L. Yang, A. G. Cruz Gonzalez, N. Tahir, M. Rini, Y.-H. Chu, R. Ramesh, D.-H. Lee, Y. Tomioka, Y. Tokura, Z. Hussain, and R. W. Schoenlein, *Phys. Rev. Lett.* **106**, 186404 (2011).
- [24] T. A. W. Beale, S. B. Wilkins, R. D. Johnson, S. R. Bland, Y. Joly, T. R. Forrest, D. F. McMorrow, F. Yakhou, D. Prabhakaran, A. T. Boothroyd, and P. D. Hatton, *Phys. Rev. Lett.* **105**, 087203 (2010).
- [25] S. Smadici, J. C. T. Lee, S. Wang, P. Abbamonte, G. Logvenov, A. Gozar, C. Deville Cavellin, and I. Bozovic, *Phys. Rev. Lett.* **102**, 107004 (2009).
- [26] J. P. Hannon, G. T. Trammell, M. Blume, and D. Gibbs, *Phys. Rev. Lett.* **61**, 1245 (1988).
- [27] J. P. Hill and D. F. McMorrow, *Acta Cryst.* **52**, 236 (1996).